Neural Correlates of Purchasing Behavior in the Prefrontal Cortex: An Optical Brain Imaging Study

Murat Perit Çakır (perit@metu.edu.tr)
METU Informatics Institute, Department of Cognitive Science
Ankara, TURKEY

Tuna Çakar (cakar.tuna@metu.edu.tr)
METU Informatics Institute, Department of Cognitive Science
Ankara, TURKEY

Yener Girişken (yener.girisken@thinkneuro.net)
Graduate School of Marketing Communications, Istanbul Bilgi University
İstanbul, TURKEY

Abstract

Existing neuroimaging studies in decision making predominantly employ the fMRI method. Despite its superior spatial resolution, fMRI is an expensive and impractical neuroimaging technology for purchasing behavior studies in the field. This study aims to explore the role of prefrontal cortex during purchasing behavior by utilizing functional near-infrared (fNIR) spectroscopy; a low-cost, non-invasive and portable optical brain imaging methodology. The findings suggest that fNIRS can be effectively used for developing a neuro-physiologically informed, predictive model of purchasing behavior based on multivariate effects of activations in frontopolar, dorso-medial and dorso-lateral prefrontal cortex.

Keywords: Neuroeconomics, neuromarketing, purchasing behavior, decision making, optical brain imaging, fNIR.

Introduction

Neuroeconomics has emerged as an interdisciplinary field to develop a better understanding of neurobiological factors that shape economic decisions (Politser, 2008). In particular, neuroeconomics research seeks to further our understanding with regards to what variables are computed by the brain while humans are making different kinds of decisions, and how those computations are implemented and constrained by underlying neurobiological processes, with the eventual goal of building biologically plausible models for human decision making (Rangel & Clithero, 2014). Existing work in the field include decision making scenarios ranging from simple decision tasks such as choosing pizza over salad for lunch to decision making under uncertain, dynamically unfolding circumstances such as gambling tasks (Glimcher & Fehr, 2014). Although these studies include rather simplistic decision making scenarios due to the limitations imposed by brain imaging tools, they collectively identified important neural mechanisms for related cognitive and emotional processes such as reward evaluation, ambiguity/risk management and value comparison (Smith & Huettel, 2010).

A number of brain imaging studies have focused on the role of the dopaminergic system in forming and updating expectations about rewards and value computation (Smith & Huettel, 2010). Monetary reward experience and evaluation processes have been found to activate several interconnected regions of this system, including the deep structures of the brain stem at ventral tegmental area (VTA) and the ventral striatum (vSTR), as well as the ventromedial prefrontal cortex (vmPFC) (Schultz, 2006; Knutson et al., 2000; Knutson et al., 2003). Especially the receipt of rewards were found to evoke activation in the vmPFC and the adjacent orbitofrontal cortex (OFC), which support the theory that these regions may be involved with computing the expected value of a reward (Knutson et al., 2005). Even activations observed at mPFC and straitum during passive viewing of products can be later used for predicting that consumer's choices involving those products (Levy et al., 2011). In a recent study, Metereu & Dreher (2015) found that the OFC/vmPFC region encodes a general unsigned anticipatory subjective value signal for both rewards and punishments.

Real world decision-making often involves uncertainty, which is another crucial factor that modulates the values attributed to choices. Imaging studies that involve uncertainties and risks in decision-making report activations in dorsolateral and lateral PFC, vmPFC, orbitofrontal cortex (OFC) and the anterior cingulate cortex (ACC) as well as subcortical regions including VTA, vSTR and amygdala (Holper et al., 2014; Smith & Huettel, 2010). This distributed neural network is claimed to encode two components of a subjective value signal, namely expected value and risk probability (Schonberg et al., 2012; Ogawa et al., 2014). The medial and lateral prefrontal cortex is claimed to play a role in integrating these two components (Tobler et al., 2009). The computations carried out in these regions are likely to be associated with subjective value signals, but not as robustly as the vmPFC/OFC regions. In particular, the dorso-lateral regions are argued to have a regulatory role on medial PFC during decision making scenarios (McClure et al., 2004). However, the precise computational roles played by the dorso-medial and dorso-lateral areas remain to be an important issue in simple choice and reward processing paradigms in neuroeconomics (Rangel & Clithero, 2014).

Existing studies in neuroeconomics predominantly employ the fMRI method. Despite its superior spatial resolution, fMRI is an expensive and impractical neuroimaging technology for purchasing behavior studies in the field. In this paper, the functional near-infrared spectroscopy (fNIRS) method was employed to study purchasing behavior, which offers a low-cost, non-invasive and portable optical brain imaging methodology. The aim of this study is to explore the plausibility of the fNIRS methodology for neuroeconomics applications, as well as to develop a neuro-physiologically informed predictive model of purchasing behavior based on fNIR measurements.

There are only a few fNIR studies published in neuroeconomics context. Existing fNIR studies have identified activation patterns in the prefrontal cortex during product selection (Kumagai, 2012), risk assessment (Holper, 2014), financial investment (Shimokawa et al., 2009) and price prediction (Mitsuda et al., 2012). Mitsuda et al. (2012) also proposed a support vector machine algorithm for classifying price/product pairings that were tagged as expensive or inexpensive by the participants with an accuracy of 70%. The present study aims to contribute this line of inquiry by investigating activation patterns in PFC of consumers during a more realistic, mundane purchasing scenario. In particular, we aimed to identify whether positive and negative purchasing decisions differ in terms of the neural activity they elicit in regions located at fronto-polar, dorso-medial and dorso-lateral prefrontal cortex.

The rest of the paper is organized as follows. The experiment design and the fNIR optical brain imaging technology employed are described in the next section. Next, we present our main findings regarding activation patterns in fronto polar, dmPFC and dlPFC regions. This section also presents a discriminant analysis model that predict the purchasing decision offline in terms of changes detected in oxy and deoxy-hemoglobin concentrations in these brain regions. The paper concludes with an overall discussion of the results.

Material and Methods

33 participants (17 female) in the age range 18-46 have participated in this experiment. They were selected randomly from the consumer database of ThinkNeuro. All participants were right-handed as measured by the Edinburgh handedness survey (Oldfield, 1971). None of the participants had a history of psychiatric disorders. Participants were paid 10 TL for their participation and 40 TL as a bonus in compensation for the items they selected to purchase during the experiment. The data of one participant has been excluded due to the fact that he has not made any buy or pass responses during the experiment. The study was approved by the METU human subjects research ethics committee. Written informed consent was obtained prior to the experiment.

The task was comprised of 78 trials where participants were asked to make purchasing decisions for the displayed products based on the suggested prices. In each block, the participants had 4 seconds for viewing a picture of the product, 4 seconds for viewing the price of the product and 4 seconds to respond according to their preference to purchase or not to purchase, followed by a fixation for 8 seconds. Each block lasted for 20 seconds. The total duration of the experiment was 26 minutes. E-Prime software was used for the presentation of the experiment stimulus. The keys participants need to press to indicate buy or pass preference were randomly switched in each block to avoid lateralization biases. The products consisted of 3 main groups (food, cleaning and personal care products). There were 39 products in the food group (e.g. milk, cheese, Coke), 17 products in the cleaning group (e.g. detergents) and 22 products in the personal care group (e.g. deodorant, shampoo, toothpaste). The prices of the products were obtained from local groceries.

The participants were told that they should press a button to indicate whether they would purchase the displayed item given its price. They were also informed that the experimenters would be able to provide them up to a total 40TL (Turkish Lira) worth of the products that they selected. Subjects were also told that if they do not spend at least 40TL, they would receive only half of the unspent amount in an effort to reinforce buying behavior.

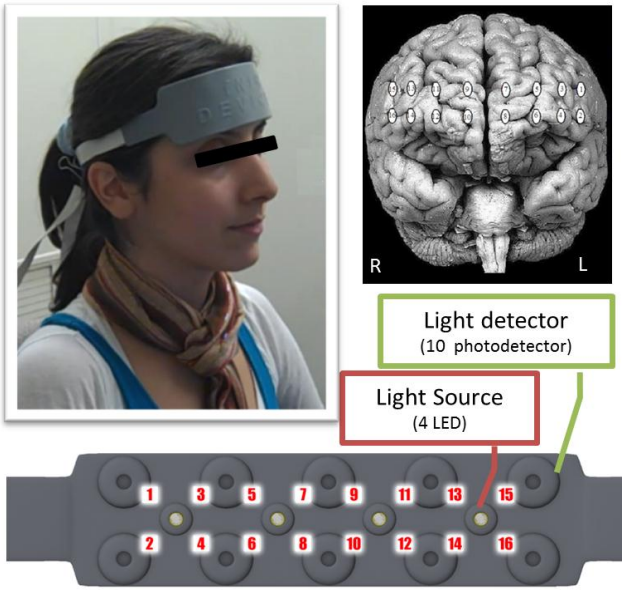

Figure 1. fNIR sensor (top, left), projection of measurement locations (optodes) on brain surface image (top, right), optodes identified on fNIR sensor (bottom).

During the experiment the prefrontal cortex of each participant was monitored with a continuous wave functional near-infrared spectroscopy (fNIR) system developed at Drexel University (Philadelphia, PA), manufactured and supplied by fNIR Devices LLC (Potomac, MD; www.fnirdevices.com). The system is composed of three modules: a flexible headpiece (sensor pad), which holds 4 light sources and 10 detectors to obtain oxygenation measures at 16 optodes on the prefrontal cortex; a control box for hardware management; and a computer that runs the data COBI Studio software (Ayaz et al., 2011) for data acquisition

(Figure 1). The sensor has a source-detector separation of 2.5cm, which allows for approximately 1.25cm penetration depth. This system can monitor changes in relative concentrations of oxy- and deoxy-hemoglobin at a temporal resolution of 2Hz. The locations of 16 regions on the cortical surface monitored by fNIR are displayed in Figure 1 above, which correspond to Broadmann areas 9, 10, 44 and 45.

fNIR is a neuroimaging modality that enables continuous, noninvasive, and portable monitoring of changes in blood oxygenation and blood volume related to human brain function. Neuronal activity is determined with respect to the changes in oxygenation since variation in cerebral hemodynamics are related to functional brain activity through a mechanism known as neurovascular coupling (Obrig et al., 2000). Over the last decade, studies in the laboratory have established that fNIR spectroscopy provides a veridical measure of oxygenation and blood flow in the brain (Bunce et al., 2006). fNIR is not only non-invasive, safe, affordable and portable, it also provides a balance between temporal and spatial resolution which makes fNIR a viable option for *in-the field* neuroimaging.

fNIR technology uses specific wavelengths of light, introduced at the scalp, to enable the non-invasive measurement of changes in the relative ratios of deoxygenated hemoglobin (deoxy-Hb or HbR) and oxygenated hemoglobin (oxy-Hb or HbO_2) in the capillary beds during brain activity. Typically, an optical apparatus for fNIR Spectroscopy consists of at least one near infra-red light source and a detector that receives light after it has interacted with the tissue. Near-infrared light is known to diffuse through the intact scalp and skull, which makes it suitable for tracing relative changes in the concentration of specific chromophores in the neural tissue with non-invasive, spectroscopic methods (Jobsis, 1977). Whereas most biological tissue (including water) are relatively transparent to light in the near infrared range between 700 to 900 nm, hemoglobin is a strong absorber of light waves in this range of the spectrum. Within 700 to 900 nm, oxy and deoxy-hemoglobin are among the highest absorbers of infra-red light. This provides an optical window into neural tissue where one can approximate relative changes in the concentration of oxy and deoxy-hemoglobin based on how infra-red light is attenuated in neural tissue.

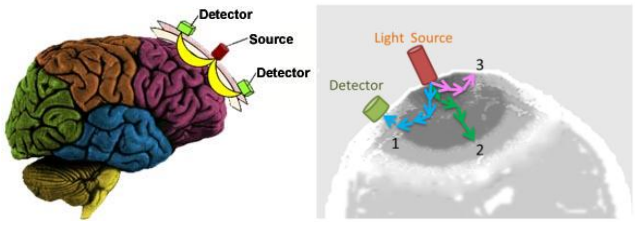

Figure 2. The banana shaped path which includes the photons scattered back to the photo-detector (left). Representative paths (right), enumerated as 2 and 3 correspond to photons absorbed by the tissue and scattered out of the scalp without reaching the detector, respectively.

Photons that enter tissue undergo two different types of interaction: absorption and scattering (Obrig et al., 2000). Two chromophores, oxy- and deoxy-Hb, are strongly linked to tissue oxygenation and metabolism. The absorption spectra of oxy- and deoxy-Hb remain significantly different from each other allowing spectroscopic separation of these compounds to be possible by using only a few sample wavelengths. Once photons are introduced into the human head, they are either scattered by extra- and intracellular boundaries of different layers of the head (skin, skull, cerebrospinal fluid, brain, etc.) or absorbed mainly by oxy- and deoxy-Hb. A photo-detector placed on the skin surface at a certain distance from the light source can collect the photons that are scattered and thus have travelled along a "banana shaped path" from the source to the detector, which carry important information about the optical properties of the diffused neural tissue (Figure 2). This raw light attenuation information is then converted into tissue oxygenation measures that quantify the relative changes in the presence of oxy- and deoxy-hemoglobin within the banana shaped path by using a method called modified Beer Lambert law (Cope et al., 1988).

Results

For each participant, buy/pass decisions, response time, total money spent and raw fNIR measures were obtained for a total of 78 grocery items. Raw fNIR data (16 optodes×2 wavelengths) were low-pass filtered with a finite impulse response, linear phase filter with order 20 and cut-off frequency of 0.1 Hz to attenuate the high frequency noise due to respiration and cardiac cycle effects (Ayaz et al., 2012). Saturated channels (if any), in which light intensity at the detector was higher than the analog-to-digital converter limit were excluded. Artifacts due to motion are detected and excluded by applying the sliding windows motion artifact filter (Ayaz, 2011). fNIR data epochs for the rest and task periods were extracted from the continuous data using time synchronization markers. Blood oxygenation changes within each 16 optodes for the product, price and decision blocks were calculated using the modified Beer-Lambert Law for task periods with respect to rest periods at the beginning of each trial with the fnirSoft software (Ayaz, 2010).

The average oxygenation level of each block was calculated and the obtained oxygenation levels for three blocks (that consist of product-price-decision) were classified according to the buy or pass decisions of the participants. The 12 sec long trials were then averaged to form evoked oxygenation (i.e. ΔHbO_2 minus ΔHbR) signals displayed in Figure 3 as a measure of brain activation. Univariate 2x3 repeated measures ANOVA conducted for each 16 voxel separately indicated that buy versus pass decisions elicit a significant difference in average oxygenation for only voxel 10, $F(1,186) = 7.65$, $p < .01$, $\eta^2 = .04$. This area corresponds to the right fronto-polar cortex, which is associated with subjective value management. No significant difference was found between product-price-purchase block types. The

interaction effect was also not significant in any of the 16 voxels.

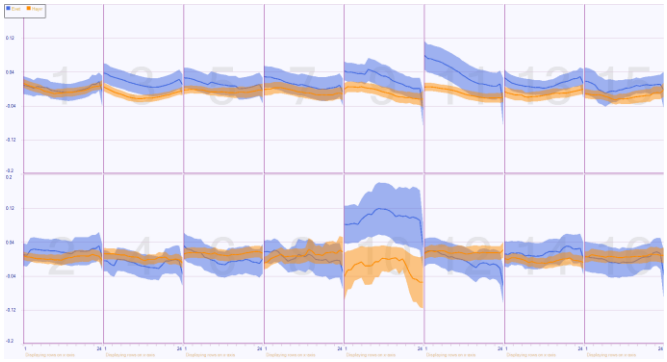

Figure 3. The temporal change in oxygenation levels (μmolar/liter) for 32 participants during the 3 blocks of 12 seconds for each 16 voxels –shown in different boxes. The blue and orange lines represent the buy and pass decisions respectively. Shades indicate standard error.

Figure 4 below shows the projection of pairwise t-statistics for each voxel with BSpline interpolation. The most significant differences in average oxygenation values are clustered around voxel 10, which is consistent with fMRI findings (e.g. Knutson et al., 2007).

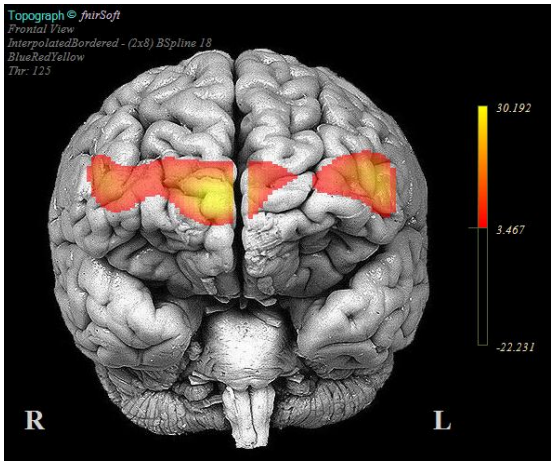

Figure 4. Projection of t-statistics map on brain surface image shows the increase in oxygenation around optode 10 during purchase decisions. BSpline interpolation was used to generate surface representation from t values of comparisons of each buy vs pass conditions along with thresholding by significance limit p<0.001 with df=24.

There was considerable variability among participants in terms of the total money they spent during the experiment (mean=95.24 TL, sd=52.38). Participants were not provided any feedback regarding the total money they spent during the experiment, and were encouraged to decide per item, even though they were informed that they could be given the products up to a total of 40TL. However, the distribution of total purchases suggest that some participants paid extra attention to their total spending. For that reason, we divided the sample into two subgroups in terms of their sensitivity to the budget limit. 11 participants who ended up spending within 20TL of the target range constitute the budget-sensitive group (mean=42.91 TL, sd=12.92), whereas the remaining 21 subjects formed the budget-insensitive group (mean=122.65 TL, sd=43.68). The analysis was repeated on these subgroups in an effort to observe if budgetary considerations made any difference in oxygenation trends.

In both of these groups, we observed that positive and negative purchasing decisions elicited higher activity in the frontopolar and dmPFC areas, albeit in different directions. Figure 5a below shows the temporal trend in average oxygenation changes observed during buy and pass decisions of the budget sensitive group. When the data of the budget-sensitive group are analyzed separately, optode 10 has been observed to preserve its significant role in the direction of buy decisions against pass decisions ($F(1,60)=18.05$, $p<.05$, $\eta^2=.23$). Moreover, there have been other optodes that appear to have significant difference including voxel 3 ($F(1,60)=11.44$, $p<.01$, $\eta^2=.16$), voxel 7 ($F(1,60)=9.46$, $p<.01$, $\eta^2=.14$), voxel 8 ($F(1,60)=10.95$, $p<.05$, $\eta^2=.15$), voxel 9 ($F(1,60)=24.37$, $p<.001$, $\eta^2=.29$), voxel 11 ($F(1,60)=18.05$, $p<.001$, $\eta^2=.23$), voxel 12 ($F(1,60)=20.42$, $p<.001$, $\eta^2=.25$), voxel 14 ($F(1,42)=4.42$, $p<.05$, $\eta^2=.20$) and voxel 15 ($F(1,54)=4.16$, $p<.05$, $\eta^2=.07$). Block type and interaction effects were not significant.

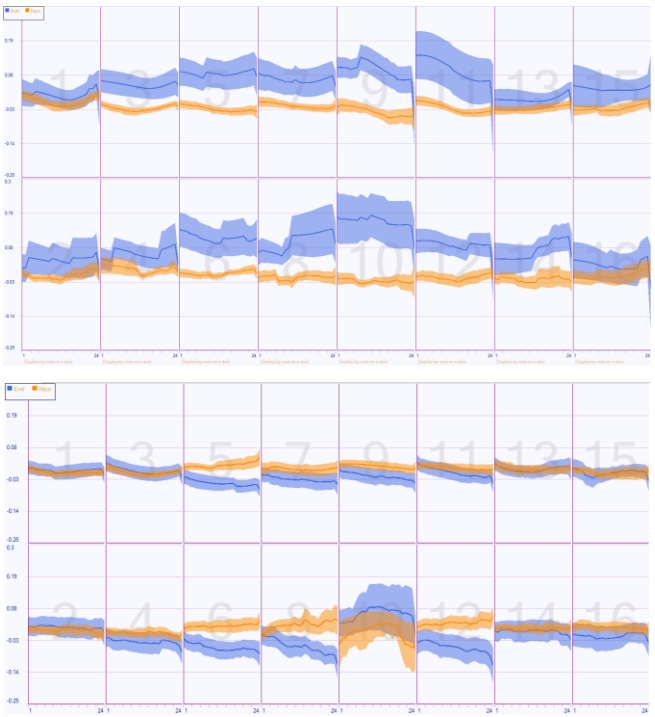

Figure 5a & 5b. The temporal change in oxygenation levels (μmolar/liter) for the budget-sensitive (top) and budget-insensitive (bottom) groups. The blue and orange lines represent the buy and pass decisions respectively. Shades indicate standard error.

When the data of budget-insensitive group composed of 21 participants are analyzed separately, significant level of

oxygenation increase has been observed for several optodes in the direction of pass decisions. These optodes include voxel 5 ($F(1,120)=14.22$, $p<.001$, $\eta^2=.11$), voxel 6 ($F(1,120)=12.96$, $p<.001$, $\eta^2=.10$), voxel 8 ($F(1,120)=8.84$, $p<.01$, $\eta^2=.07$) and voxel 12 ($F(1,120)=9.72$, $p<.01$, $\eta^2=.08$). Figure 5b shows the temporal trend in average oxygenation changes observed during buy and pass decisions of the budget insensitive group. Finally, block type and interaction effects were not significant in this group as well. To sum up, the temporal trend of average oxygenation values exhibit a different pattern across budget sensitive and insensitive groups.

Table 1. The discriminant function coefficients and the predictive success of each model.

	All Sample (N=32)	Within Budget (N=11)	Excess Budget (N=21)
Voxel 3	,408	-,344	-,462
Voxel 5	-,944	,081	1,816
Voxel 6	-,291	,007	,819
Voxel 7	,492	,025	-2,173
Voxel 8	,109	,376	,594
Voxel 9	,622	,673	,804
Voxel 10	,424	,444	,023
Voxel 12	-,851	,068	-,066
Voxel 13	,263	,136	-,202
Voxel 14	,530	-,078	-,901
Wilk's Lambda	0.82	0.58	0.48
Chi-Square	$\chi^2(10)=$ 25.56 p<.01	$\chi^2(10)=$ 22.51 p<.05	$\chi^2(10)=$ 61.53 p<.001
Purchase Centroid	0.461	-0.837	1.036
No Purchase Centroid	-0.461	0.837	-1,036
% Classified Correctly	62%	82%	74%

Related fMRI work has reported on the prominent role of the functional connectivity between medial PFC and dlPFC on the modulation of economic decisions (Ogawa et al., 2014). Since our findings from fNIR suggest differential temporal trends in oxygenation for our subgroups and the measurement locations include some of the functionally connected regions of interest in frontopolar, dorsomedial and dorsolateral sites, we also employed multivariate methods to observe if buy/pass decisions can be distinguished based on multivariate trends across multiple channels. For that purpose, a 2x3 MANOVA was performed on the oxygenation levels for the voxels 7,8,9,10 (left and right fronto-polar cortex), voxels 5-6 (left dmPFC), voxels 12-13 (right dmPFC) and voxels 3-14 (left and right dlPFC). The MANOVA results indicate significant difference for both the budget-sensitive ($F(10,33)=2.49$, $p<.05$, Pillai Trace=.43) and budget-insensitive groups ($F(1,75)=8.56$, $p<.01$, Pillai Trace=.53). The results have also been significant for the entire sample ($F(10,123)=2.67$, $p<.01$, Pillai Trace=.18). Block type and interaction effects were not significant.

The MANOVA analysis was followed up with a discriminant analysis to observe how buy and pass decisions differ from each other. The discriminant analysis was performed on the whole group as well as on the budget subgroups. In each group, a single variate was found to significantly distinguish buy and pass decisions, whose coefficients are presented in Table 1.

Table 1 suggests that when budget sensitivity is not taken into account, buy or pass decisions can be predicted with 62% accuracy, which is above chance level. When additional information about budgetary sensitivity is provided, the expected predictive accuracy can be estimated as $\frac{11}{32} * 0.82 + \frac{21}{32} * 0.74 = 0.77$. Oxygenation trend across fronto-polar, dmPFC and dlPFC regions have a higher discriminating role for the participants who paid attention to the budget limitation.

Discussion

The obtained results bear similarities with findings of existing fMRI studies in frontopolar regions. Positive purchasing decisions significantly increase the neural activity through frontopolar regions, which are closely related to OFC and vmPFC that modulate the computation of subjective values. Frontopolar regions such as voxel 10 remain to be activated in a similar way across budget sensitive and insensitive subgroups, which support the general role attributed to the OFC and its projections in the frontopolar cortex for subjective value computation.

Our results also suggest that the general purchasing tendency of the participants can significantly alter some of the activation patterns observed in other parts of the prefrontal cortex. Products ended up being purchased tend to elicit strong activation in voxel 10 as compared to other prefrontal regions. In the budget sensitive group, this activation trend had to remain strong as compared to dmPFC and dlPFC activations until the end of a trial to elicit a buy decision. In the budget insensitive group, voxel 10 activity remains high during buy decisions as well. No purchase cases also elicit comparable level of activity in voxel 10, which tend to drop towards the end of a trial together with an increase in activation in voxels 5,6 and 12 located in dmPFC. These dmPFC sites seem to inhibit the tendency to purchase in the budget insensitive group, as it was evidenced in the oxygenation trend observed during no purchase cases for the budget insensitive group. In the budget sensitive group increase in dmPFC activity has a reverse role, where it correlates with buy rather than pass decisions.

These findings implicate that the neurophysiological modeling of purchasing decisions cannot be based solely on increased neural activity in frontopolar regions. When the participants were classified according to their budget sensitivity, the predictive accuracy of the model has increased

from 60% to 80%. The difference among these two groups might be related to differences in their working memory capacities for keeping the budget constraint as part of their goal state. dmPFC is particularly involved with goal maintenance and response selection processes, which seem to contribute to the differences observed between these groups.

In conclusion, this study demonstrated that fNIR can be used to monitor activations in the prefrontal cortex during purchasing decisions. Moreover, multivariate analysis techniques can be effectively employed on oxygenation trends to build predictive computational models with reasonable accuracy. In the future, we aim to better exploit the portability of fNIR to explore neural underpinnings of economic decisions in more ecologically valid contexts.

References

Ayaz, H., Izzetoglu, M., Platek, S. M., Bunce, S., Izzetoglu, K., Pourrezaei, K., & Onaral, B. (2006). Registering fNIR data to brain surface image using MRI templates. In *28th Annual International Conference of Engineering in Medicine and Biology Society.* (pp. 2671-2674). IEEE.

Ayaz, H. (2010). *Functional Near Infrared Spectroscopy based Brain Computer Interface*, Unpublished Doctoral Dissertation, Drexel University, Philadelphia, PA, USA.

Ayaz, H., Shewokis, P. A., Curtin, A., Izzetoglu, M., Izzetoglu, K., & Onaral, B. (2011). Using MazeSuite and fNIR to study learning in spatial navigation. *JoVE*, (56).

Ayaz, H., Shewokis, P. A., Bunce, S., Izzetoglu, K., Willems, B., & Onaral, B. (2012). Optical brain monitoring for operator training and mental workload assessment. *Neuroimage*, *59*(1), 36-47.

Bunce, S. C., Izzetoglu, M., Izzetoglu, K., Onaral, B., & Pourrezaei, K. (2006). Functional near-infrared spectroscopy. *Engineering in Medicine and Biology Magazine, IEEE*, *25*(4), 54-62.

Cope, M., Delpy, D. T., Reynolds, E. O. R., Wray, S., Wyatt, J., & Van der Zee, P. (1988). Methods of quantitating cerebral near infrared spectroscopy data. In *Oxygen Transport to Tissue X* (pp. 183-189). NY: Springer.

Glimcher, P. W., & Fehr, E. (Eds.) (2014). *Neuroeconomics: Decision making and the brain*. New York, NY: Academic Press.

Holper, L., ten Brincke, R. H., Wolf, M., & Murphy, R. O. (2014). fNIRS derived hemodynamic signals and electrodermal responses in a sequential risk-taking task. *Brain Research*, *1557*, 141-154.

Jobsis, F. F. (1977). Noninvasive, infrared monitoring of cerebral and myocardial oxygen sufficiency and circulatory parameters. *Science*, *198*(4323), 1264-1267.

Knutson, B., Westdorp, A., Kaiser, E., & Hommer, D., FMRI visualization of brain activity during a monetary incentive delay task. *Neuroimage*, *12*(1), 20-27, (2000).

Knutson, B., Fong, G., Bennett, S., Adams, C., & Hommer, D. (2003). A region of mesial prefrontal cortex tracks monetarily rewarding outcomes: characterization with rapid event-related fMRI. *Neuroimage*, *18*(2), 263-272.

Knutson, B., Taylor, J., Kaufman, M., Peterson, R., & Glover, G. (2005). Distributed neural representation of expected value. *J. of Neuroscience*, *25*(19), 4806-4812.

Knutson B., Rick S., Wimmer G.E., Prelec D., Loewenstein, G. (2007). Neural Predictors of Purchases, *Neuron*, *53*, 147-56.

Kumagai, M. (2012). Extraction of personal preferences implicitly using NIRS. In *Proceedings of IEEE SICE Annual Conference (SICE 2012)* (pp. 1351-1353).

Levy, I., Lazzaro, S. C., Rutledge, R. B., & Glimcher, P. W. (2011). Choice from non-choice: predicting consumer preferences from blood oxygenation level-dependent signals obtained during passive viewing. *The Journal of Neuroscience*, *31*(1), 118-125.

McClure, S. M., Li, J., Tomlin, D., Cypert, K. S., Montague, L. M., & Montague, P. R. (2004). Neural correlates of behavioral preference for culturally familiar drinks. *Neuron*, *44*(2), 379-387.

Metereau, E., & Dreher, J. C. (2015). The medial orbitofrontal cortex encodes a general unsigned value signal during anticipation of both appetitive and aversive events. *Cortex*, *63*, 42-54.

Mitsuda, Y., Goto, K., Misawa, T., & Shimokawa, T. (2012). Prefrontal cortex activation during evaluation of product price: A NIRS study. In *Proc. of the Asia Pacific Industrial Engineering & Management Systems Conference*.

Obrig, H., Wenzel, R., Kohl, M., Horst, S., Wobst, P., Steinbrink, J. & Villringer, A. (2000). Near-infrared spectroscopy: does it function in functional activation studies of the adult brain? *International Journal of Psychophysiology*, *35*(2), 125-142.

Ogawa, A., Onozaki, T., Mizuno, T., Asamizuya, T., Ueno, K., Cheng, K., & Iriki, A. (2014). Neural basis of economic bubble behavior. *Neuroscience*, *265*, 37-47.

Oldfield, R. C. (1971). The assessment and analysis of handedness: the Edinburgh inventory. *Neuropsychologia*, *9*(1), 97-113.

Politser, P. (2008). *Neuroeconomics: A guide to the new science of making choices*. New York, NY: OUP.

Rangel, A., & Clithero, J. (2014). The computation of stimulus values in simple choice. In P. Glimcher & E. Fehr (Eds) *Neuroeconomics: decision making and the brain*, (*2nd Ed)* (pp. 125-148). New York, NY: Academic Press.

Schultz, W. (2006). Behavioral theories and the neurophysiology of reward. *Annu. Rev. Psych.*, *57*, 87-115.

Shimokawa T., Misawa T., Suzuki K. (2008). Neural Representation of Preference Relationships, *NeuroReport*, *19*, 1557-61.

Smith, D. V., & Huettel, S. A. (2010). Decision neuroscience: neuroeconomics. *Wiley Interdisciplinary Reviews: Cognitive Science*, *1*(6), 854-871.

Tobler, P. N., Christopoulos, G. I., O'Doherty, J. P., Dolan, R. J., & Schultz, W. (2009). Risk-dependent reward value signal in human prefrontal cortex. *PNAS*, *106*(17), 7185-7190.